energies

MDPI

Article

Emissions Performance of the Hydrogen–Methane Blends for Buses During Real Driving Tests

Federico Di Prospero *, Marco Di Bartolomeo, Davide Di Battista * and Roberto Cipollone

Department of Industrial and Information Engineering and Economics, University of L'Aquila, P.le Pontieri 1, 67100 L'Aquila, Italy; marco.dibartolomeo2@univaq.it (M.D.B.); roberto.cipollone@univaq.it (R.C.)

* Correspondence: federico.diprospero@graduate.univaq.it (F.D.P.); davide.dibattista@univaq.it (D.D.B.); Tel.: +39-0862-434338 (F.D.P.)

Abstract

The transportation sector, a major source of urban air pollution and CO_2 emissions, is the focus of extensive research aimed at developing cleaner and more efficient technologies. In this context, hydrogen–methane blends (HCNG) represent a promising alternative fuel, combining the zero-carbon combustion potential of hydrogen with the availability and cleaner profile of methane. This solution can be implemented in existing internal combustion engines, enabling a technically and economically feasible transition toward more sustainable mobility. This work investigates the use of an HCNG blend in a bus originally powered by natural gas, focusing on pollutant emissions under real driving conditions representative of typical urban operation. Measurements were performed using a Portable Emission Measurement System installed on-board. Two test campaigns were carried out: the first using methane, and the second using an HCNG blend (15% H_2, 85% CH_4 by volume), over identical urban and extra-urban routes with varying drivers and traffic conditions. Results show a reduction in CO_2 emissions with HCNG, along with a more significant decrease in CO, HC, and PN emissions, while NOx exhibited a slight increase due to unchanged engine calibration. The analysis also includes the RPA index, which is related to fuel energy release characteristics, indicating improved vehicle responsiveness and torque delivery with HCNG.

Keywords: HCNG; hydrogen; CNG; internal combustion engine; emissions reduction; emissions; RPA index; HCNG fuel

1. Introduction

The European Green Deal, announced by the European Commission in 2019, represents a transformative policy aimed at making the European Union the first climate-neutral region by 2050 [1]. A central element of this ambitious objective is decarbonization. The ecological transition represents one of the major challenges of contemporary society and requires a substantial change in energy consumption patterns to mitigate the global climate emergency. Greenhouse gas emissions, which are strongly correlated with energy use [2], involve all economic sectors, including transportation, which ranks as the second most energy-intensive sector worldwide [3], accounting for approximately 27% of global primary energy consumption [4]. Within this sector, the road transport of passengers and goods represents the predominant share, at approximately 75% [5]. In response, governments have introduced CO_2 reduction targets, accompanied by economic penalties in case of non-compliance. Although the 2021 targets in the European Union (EU) were achieved, thanks

Academic Editor: Marian Banaś

Received: 6 April 2026
Revised: 24 April 2026
Accepted: 29 April 2026
Published: 2 May 2026

to emission reductions related to the COVID-19 pandemic [6], the 2030 targets will require significant technological innovations and a stronger effort, not only technological. Consequently, it is necessary to improve vehicle energy efficiency—by reducing fuel consumption and well-to-wheel emissions and use fuels with a reduced carbon content—to mitigate their negative climate impact [7]. Vehicles powered by internal combustion engines (ICEs) remain one of the main sources of air pollution, especially in urban and suburban areas where people live. Since the early 1990s, increasingly stringent emission regulations, currently culminating in the forthcoming Euro 7 regulation [8], have reduced major pollutants such as CO, HC, NOx and PM by approximately 90% compared to pre-regulation levels [9], thanks to targeted research and the implementation of exhaust after-treatment technologies, which enable their abatement. In this historical period, the sector is undergoing a profound technological evolution, characterized by the integration of traditional internal combustion engines (ICEs) with electric and hybrid propulsion systems [10,11].

Hybridization and electrification currently represent two of the main strategies for reducing the environmental impact of road transport and have already achieved a certain level of market penetration within the European Union [12]. Battery-powered electric vehicles allow the elimination of tailpipe emissions, with direct benefits on urban air quality, especially if powered by renewable sources [13]. However, CO_2 emissions are partially transferred upstream in the energy supply chain, particularly in contexts where the electricity mix still depends on fossil fuels [14]. Although electrification is progressively transforming the light-duty vehicle segment, the application of fully electric solutions to heavy-duty vehicles (HDVs) remains challenging in the short term. This is due to several factors that still limit the large-scale deployment of electric vehicles, primarily limited driving range, long charging times, and dependence on rare and costly materials for motors and batteries (rare earths, lithium, etc.) [15–17]. A care should also be considered in those countries where the carbon intensity of the electricity (available on the grid gCO_2/kWh) is over a certain limit, being the mix of it generated using high carbon content fuels, which is more frequent than one might expect. It is a common opinion between engine manufacturers, researchers and market experts that electrification is a good answer to passenger and light-duty vehicles, while in the heavy-duty sector decarbonization has also to follow other directions, mainly those oriented to the fuel/energy vector. Moreover, in heavy-duty vehicles, the high power density [18] makes proper thermal management essential to prevent component degradation, loss of efficiency, and reduced service life [19], rediscovering again the importance of technological advancements referred to engine/motor and/or battery cooling [20–23], energy optimization, hybridization finalized to braking energy recovery, propulsion power reduction, etc.

In this transition scenario, technologies capable of improving energy efficiency and reducing emissions while maintaining the conventional architecture of internal combustion engines play a strategic role. In this context, waste heat recovery (WHR) represents one of the most promising solutions, both in conventional and hybrid systems [24], where the recovered energy can be stored and used to power electrical appliances [25,26]. Many research programs have confirmed the key role of WHR in achieving high-efficiency goals [27,28]. In general, waste heat recovery can be achieved through Direct Heat Recovery (DHR) [29], Indirect Heat Recovery (IHR) [30], or mixed [31] heat recovery approaches. Turbo-compounding represents one of the most mature DHR technologies, allowing the recovery of exhaust gas energy, although careful design [32] is required to mitigate drawbacks such as increased exhaust backpressure [33]. Among IHR systems, organic Rankine cycle (ORC) technologies are widely studied for their flexibility and operational stability [34], although their diffusion is limited by the highly transient thermal conditions typical of

road vehicles and the quantity of required components, related to weight and required space allocation [35,36].

At the same time, engine thermal management technologies are becoming increasingly important, aimed at both increasing efficiency and reducing emissions [37]. The evolution of traditional cooling systems towards more integrated and controllable solutions [38], the optimization of intake air cooling [39] and the active regulation of the coolant flow rate through specifically redesigned electric pumps [40] allow for a more precise control of operating conditions, improving overall performance. Strategies to accelerate the heating of the lubricating oil are also essential to reduce friction, consumption and emissions during cold start phases [41].

In the urban transport means panorama, diesel engines are by far the most used ones, but with climate impact and air pollution in cities issues [42]. Alternatives to diesel engines are more than welcome [43], but the replacement with battery vehicles, as stated, is very difficult and the use of low-carbon fuels [44] can preserve the present technology, favoring a more gradual transition. Alternative fuels [45,46], biofuels [47,48], methanol [49], or e-fuels [50] are playing an increasingly important role [51], although careful consideration of the entire driving cycle remains necessary [52]. Alternative gaseous fuels such as CNG and hydrogen tend to reduce combustion-related noise compared to diesel engines, mainly due to more homogeneous charge formation; however, the magnitude of this effect depends on operating conditions and engine configuration [53].

Among these options, hydrogen emerges as a particularly promising energy carrier, since its carbon-free chemical composition allows the elimination of CO_2 tailpipe emissions, both in fuel cell applications and in internal combustion engines specifically designed for hydrogen use [54]. Hydrogen is the most abundant element, accounting for approximately 75% of matter; however, its abundance on Earth is much lower, around 0.2% by mass, with most of it bound to oxygen in water [55]. Compared to hydrocarbon fuels, hydrogen has the advantage of a lower heating value of about 120 MJ/kg [56], which is 2.5 times that of methane and nearly three times that of gasoline and diesel fuel [57]; consequently, its high energy yield makes H_2 a highly important energy carrier. Currently, approximately 70–80 tons of H_2 are produced annually for industrial uses alone [58], and its use as a fuel remains relatively marginal, although H_2 can be used to power fuel cells (FCs) to drive electric traction motors [59–61], representing a direct alternative to battery electric vehicles (BEVs). From the study of hydrogen in bus traction engines, from a theoretical point of view, together with DHR strategies, significant fuel saving advantages amounting to almost 7% are found [62]. Despite the market availability of some models, including buses [63,64], deployment remains limited due to the complexity of distribution and refueling infrastructures [65], as well as challenges related to on-board storage [66,67]. Moreover, hydrogen's high flammability and flame temperature pose challenges for direct combustion, leading to increased NOx emissions and often requiring combustion chamber modifications [68,69]. Very lean mixture during combustion is required to mitigate the high energy content which entrains a very fast flame propagation (having an explosive nature) as well as to depress the NOx formation.

Hydrogen can be blended with natural gas up to a maximum of 15% by mass, contributing to a reduction in fuel CO_2 intensity [70]. Natural gas remains a valid alternative to conventional fuels due to its lower carbon-to-hydrogen ratio compared to petroleum-derived fuels [71]. Vehicles powered by compressed natural gas (CNG) allow reductions in emissions, particularly particulate matter; however, intrinsic CNG limitations, such as low flame speed and narrow flammability range, can compromise combustion efficiency under lean operating conditions [72–74]. Compressed natural gas (CNG) vehicles are regulated within the same general framework as conventional spark ignition vehicles, particularly in

regions such as the European Union, where emission standards define limits for key pollutants including CO, NOx, hydrocarbons (HCs), and particulate matter. CO_2 regulation also applied to CNG engines [75]. However, recent regulatory discussions highlight important limitations. While CNG performs well for regulated pollutants, it raises concerns regarding unregulated or weakly regulated species, particularly methane (CH_4), ammonia (NH_3), and nitrous oxide (N_2O). These emissions are increasingly relevant because methane is a potent greenhouse gas [76] when it is emitted directly as unburned species. Incidentally, the use of natural gas as fuel for buses operating in urban areas today represents the most used answer to air quality improvements and decarbonization, being considered the most appropriate technological evolution of the previous diesel fuel propulsion. It is not of secondary importance that this choice allows us to favor, in a sector particularly critical as alternatives, a transition toward a zero-carbon emission which cannot be disruptive for social and other related aspects concerning a more complete sustainability concept.

In this context, hydrogen-enriched compressed natural gas (HCNG) emerges as a promising transitional fuel toward a hydrogen economy. HCNG blends combine the advantages of CNG with hydrogen's superior combustion properties, including high laminar flame speed, wide flammability limits, and cleaner combustion products [77–80]. An additional advantage of HCNG lies in its potential use in existing CNG engine platforms with relatively limited modifications, enabling a gradual and cost-effective transition [81]. Experimental studies and recent technological developments indicate that HCNG fueling improves engine thermal efficiency, reduces exhaust emissions, and enhances combustion stability under lean conditions, making it a sustainable solution in both the short and medium-to-long term [82–84]. However, the optimization of the hydrogen fraction in the blend is crucial. Moderate enrichment levels (18–25% by volume) provide significant benefits [85], whereas higher fractions (above 30%) may cause combustion instabilities such as preignition, backfire, and increased thermal loads [71,86].

In this study, pollutant emissions from a bus used for urban public transportation were compared. The bus chosen is a Solaris Urbino Keolis 12 m natively powered by CNG. The emission comparison is based on on-road tests. Emissions were evaluated when the vehicle was fueled with both methane and a HCNG blend. Comparisons were carried out on both urban and extra-urban routes. To enable this, the bus was partially modified along the exhaust line to allow easier interception of exhaust gas flow compared to the original configuration. Following this modification, the vehicle was instrumented. An AVL PEMS gas analyzer was installed on-board. The analyzer consists of multiple modules, each suitable for measuring and quantifying a specific pollutant species. It was installed together with all the instrumentation required for operation and data acquisition. Two different routes, one urban and the other extra-urban, were selected, considering all aspects necessary for successful test execution. The novelty is related to the real driving tests effectuated, that aimed at demonstrating the real emission reduction on the road of the HCNG blend. Moreover, these tests were made without any change in system powertrain, injection, or control strategies, assessing the potentiality of 15% hydrogen drop-in enrichment in conventional CNG at zero cost. The choice to make reference to real driving instead of considering a homologation RDE test was due to verifying the environmental effectiveness on the road, which often presents engine operating conditions as being more critical than those considered in the approval tests (in terms of weight increase, instantaneous accelerations, irregular stops and starts, air quality aspirated by the engine, driving style, etc.). All these aspects led the authors to believe that any improvements measured on the road would have been more significant (or equally significant) than those evaluated in a homologation RDE test.

Experimental campaigns were first conducted using methane without modifying the fuel storage system, followed by campaigns using HCNG, which required modifications to the storage system. During the tests, vehicle speed and distance travel were recorded. Pollutant emissions including CO_2, CO, HC, NOx, and PN were measured. Measurements were not continuous; the sampling frequency was 1 Hz, corresponding to one measurement per second. For each test, cumulative emissions were calculated and used for comparison, expressed both per kilometer and per kilowatt-hour of energy. Results show that CO_2, CO, HC, and PN emissions decrease when HCNG is used, while NOx emissions increase, in agreement with the literature data. Subsequently, the RPA index was calculated for all tests, showing improved engine performance when fueled with HCNG, consistent with driver feedback. In both cases when pure methane and HCNG were used as fuel, the injection parameters were kept unchanged with respect to the pure methane use to favor the criterium of a simple methane replacement.

2. Materials and Methods

A road test was conducted with a bus used for public transport in the Abruzzo Region owned by TUA S.P.A, located in Pescara, Italy. Real-world driving tests (RDE) were conducted with both the methane-powered bus and the HCNG-powered bus. No substantial changes were made to the engine mapping to safely transition from CNG to a 15% HCNG blend. The chosen bus is a 12 m Solaris Urbino Keolis natively powered by CNG, as shown in Figure 1.

Figure 1. Solaris Urbino 12 CNG Keolis bus used for road tests.

The bus considered is powered by natural gas ICE (CNG—compressed natural gas) with a gas composition typical of the national network; it is 12 m long and falls into the M3 Class I category, having more than 8 seats (excluding the driver's seat). It has a maximum mass exceeding 8 t and is equipped with both seats and standing room. In Table 1, the most important technical data on the bus is reported.

Table 1. Technical data of the engine and the bus used for the tests.

Parameter	Value
Model Name	Solaris Urbino 12 CNG
Category	M3
Class	I
Kerb Weight [kg]	11,970
Gross Vehicle Weight (GVW) [kg]	19,000
Length [m]	12
Width [m]	2.55
Height [m]	3.433
Number of Axles	2
Seating Capacity	30
Standing Capacity	64
Engine	Iveco Cursor 8 Inline 6-Cylinder, spark ignition
Valvetrain	24 valves, overhead camshaft
Rated power	290 HP

2.1. Instrumentation Used for Data Acquisition

The system used for pollutant detection consists of several modules:

- Gas PEMS iS+: This instrument measures the concentration of CO, CO_2, NO_2, NO, and O_2 in exhaust gases.
- PN PEMS iS+: This instrument measures the concentration of particulate matter in exhaust gases; this module was designed to detect the number of particles in exhaust gases.
- MOVE EFM: It measures exhaust gas flow with the software AVL Concerto 6.3. The acquisition system used is the flow integration module.
- Flowmeter: This hardware component enables measurement.
- E-BOX iS+ (also called Power Distribution): Distributes the necessary power to all components.
- System control: It communicates with all modules and records data.
- Battery: Provides power to all components during the test.
- Charge Master: Recharges the battery and provides power to all modules during the pre-test and post-test.
- FID iS+: This instrument measures the HC concentration in exhaust gases through the FID data acquisition module.
- Ecal: Calibration module.

System control constitutes the core of the system: all the exhaust gas analysis instruments send data to this unit, which is visible through the data acquisition software named AVL Concerto (property of the manufacturer) on a connected PC. It is also responsible for storing all data from the measuring instruments, the GPS system, and the vehicle's ECU. The system control unit is connected to the e-Box for distributing the necessary power to all components, which is connected to the two batteries and the pollutant measurement devices, respectively. The instrumentation used for the measurement of polluting species has the characteristics reported in Table 2. The polluting species analyzed, the measurement range, the accuracy, the precision and the linearity in the measurement are reported.

Table 2. Instrumentation measurements characteristics.

Instrumentation Measurements Characteristics				
Gas Analyzed	**Measuring Range**	**Accuracy**	**Precision**	**Linearity**
CO	0–50,000 ppm	0–1499 ppm: ±30 ppm 1500–50,000 ppm: ±2% rel.	1% F.S.	0.99% ≤ Slope ≤ 1.01 Intercept = 0.5% SEE: ≤1% of range and $R^2 \geq 0.999$
CO_2	0–20% vol	±0.3% F.S. o ±2% rel.	1% F.S.	
NO	0–5000 ppm	±0.2% F.S. o ±2% rel.	0.5% F.S.	
NO_2	0–2500 ppm	±0.2% F.S. o ±2% rel.	0.5% F.S.	
O_2	0–25% vol	±1% vol F.S. for temperature and pressure constant		
THC	0–30,000 ppm C1	±5 ppm C1 or 0.3% F.S.	-	0.99% ≤ Slope ≤ 1.01 Intercept = 0.5% SEE: ≤1% of range and $R^2 \geq 0.999$
CH_4	0–10,000 ppm C1		-	

2.2. On-Board Installation

For the tests, no modifications were made to the vehicle, except for the exhaust line, which was intercepted after the catalytic converter and modified by removing the original pipe and inserting a new one with a different route so it could be connected to the instrumentation used. The new pipe also included a location for the lambda probe to ensure the closed-loop control function. The installation of the PEMS modules and the new exhaust line are shown in Figure 2.

Figure 2. Real photos taken on the bus that show the system used for data acquisition with the components necessary for its operation and the modified exhaust line.

2.3. Storage and Filling of HCNG Tank and HCNG Management

Firstly, the experimental operation used conventional CNG fuel, followed by a pre-prepared hydrogen–methane (HCNG) blend containing 15% hydrogen by volume. The fuel was stored in tanks for a total of 1600 L of fuel. The initial pressure at which the two-cylinder packs were filled was 200 bars, at an ambient temperature of 20 °C.

The bus used for the tests was equipped with six 214 L tanks, for a total capacity of 1284 L, with a maximum operating pressure of 200 bar and a minimum operating pressure of 40 bar. However, only three of the six were loaded with HCNG. A reserve of CNG was kept in the other three to power the bus in the event of a misfunction or the HCNG mixture. It should be noted, however, that the three tanks loaded with methane were closed and did not contribute to the vehicle's fueling during the tests.

The HCNG refilling operations were carried out by pressure differential through a hydrogen-compatible hose.

The architecture of the powertrain was not changed; in fact, the powertrain architecture was not modified for HCNG operation. The engine operates under stoichiometric conditions with port fuel injection. The HCNG blend (15% vol. hydrogen, 85% natural gas) was prepared externally and used as a direct replacement for conventional CNG, without requiring any changes to the engine hardware or ECU control strategy.

2.4. Test Mode

Tests are performed as illustrated in Figure 3. The preparation phase consists of assembling the equipment, checking that all modules are connected correctly, and entering the vehicle parameters (category, engine size, name of the experiment).

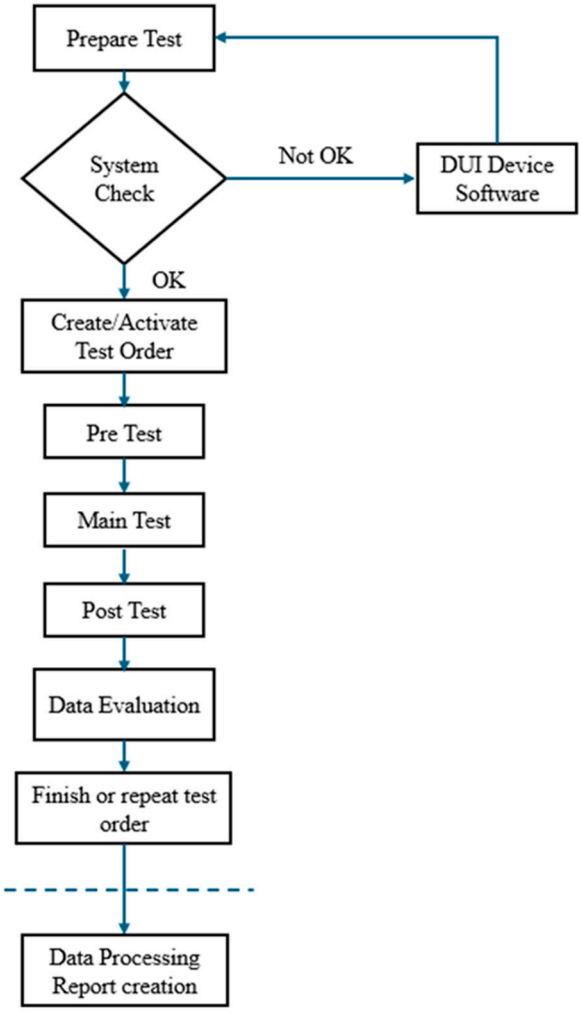

Figure 3. Logical diagram of the test's operations.

The check phase makes it possible to verify that communication between the various modules is occurring correctly. All components are controlled remotely via the PC

connected to the system control, and proper connection can be verified by examining the pollutant values detected by the instruments. The same operation must be repeated to verify the OBD connection. The test must then be created and activated (activation phase).

The pre-test phase continues, which consists of verifying the internal functionality and calibrating the measurement range of the individual modules. The checks performed include:

- Purges, which are purging the modules' internal ducts to minimize contamination of the samples collected and avoid damaging the machinery;
- Leak checks, which are a check of the tightness of the internal pneumatic circuits; if this check fails, it means that one or more circuits have not been connected correctly and there is the possibility of aspirating ambient air, which would contaminate the exhaust gas samples;
- Zero adjusts, which consist of setting the zero of the measurement range for each module by sending calibration gases to the instrumentation that do not contain the pollutant for which the instrumentation was designed;
- Span adjustments consist of setting, for each module, a point within the measurement range. They are performed by sending calibration gases with well-defined concentrations to the instruments.

The main test phase then proceeds, which involves continuously measuring pollutants while the vehicle is in motion. All signals from the individual modules and the vehicle itself can be monitored via OBD on the on-board PC.

This is followed by the post-test, in which the purges (discussed in the pre-test), zero checks, and span checks are performed again using the previously described methods. These checks are used to determine whether the instrumentation lost the calibration during the main test and, if necessary, correct it during data analysis.

The data can be checked (data evaluation) to ensure no steps have been missed, and the test can be concluded (finish test order). Each check of the various phases is recorded in the test report, and it is possible to verify that they have been successfully passed.

2.5. Route Selection

Two main factors had to be considered when choosing the route:

- The limited battery life of the PEMS batteries, which lasts approximately 2 h; after this time, they must be reconnected to the charger and then to a power outlet.
- The blend used (15% hydrogen and 85% methane by volume) has slightly higher energy content and therefore a higher calorific value than methane alone. Since it was decided not to change anything to the engine (for example, adjusting the ignition timing), to always perform the tests with a high degree of safety, as a precaution, the route will not have excessive gradients to limit engine strain.

Given the above considerations, two routes were chosen:

- An urban one 13 km long, and a journey time of approximately 45 min.
- An extra-urban one 18 km long, and a journey time of just over 20 min.

Tests were repeated under different traffic conditions during the days, with different drivers and weather conditions. Then they are grouped and averaged values calculated, to reduce the influence of the variability of external factors on the on-the-road results and giving higher reliability to the measures.

3. Results and Discussion

The road tests were divided into two groups, both by the type of route taken and the fuel used to power the vehicle. The chosen urban route shown in Figure 4a covers 13 km, while the extra-urban route shown in Figure 4b covers 18 km. Each route was repeated

several times, both with the methane-fueled vehicle and the HCNG-fueled vehicle. In both cases, the altitude of the route remains almost unchanged.

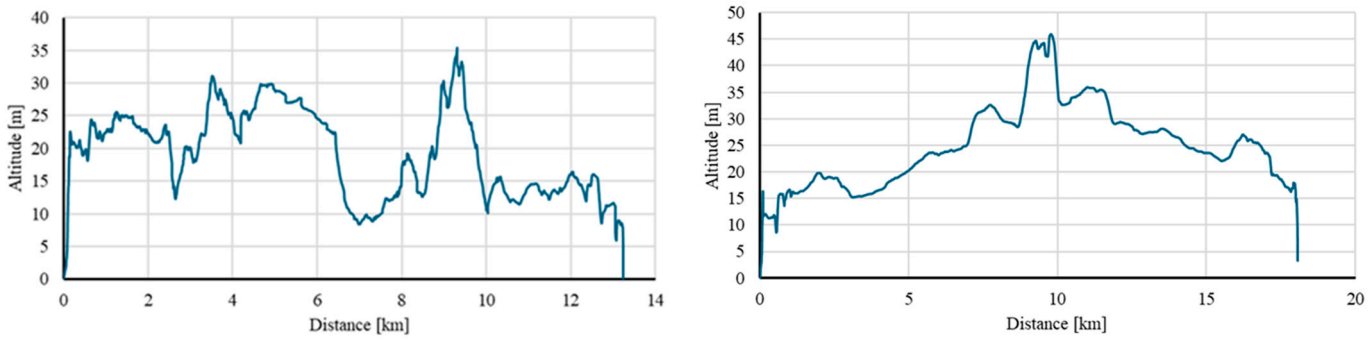

(**a**) Urban test (**b**) Extra-urban test

Figure 4. Altitude profile of the urban (**a**) and extra-urban (**b**) route.

3.1. Speed Profile

Figure 5a–d show the vehicle's speed profile during each road test. The vehicle's speed was detected by the GPS positioned on the vehicle.

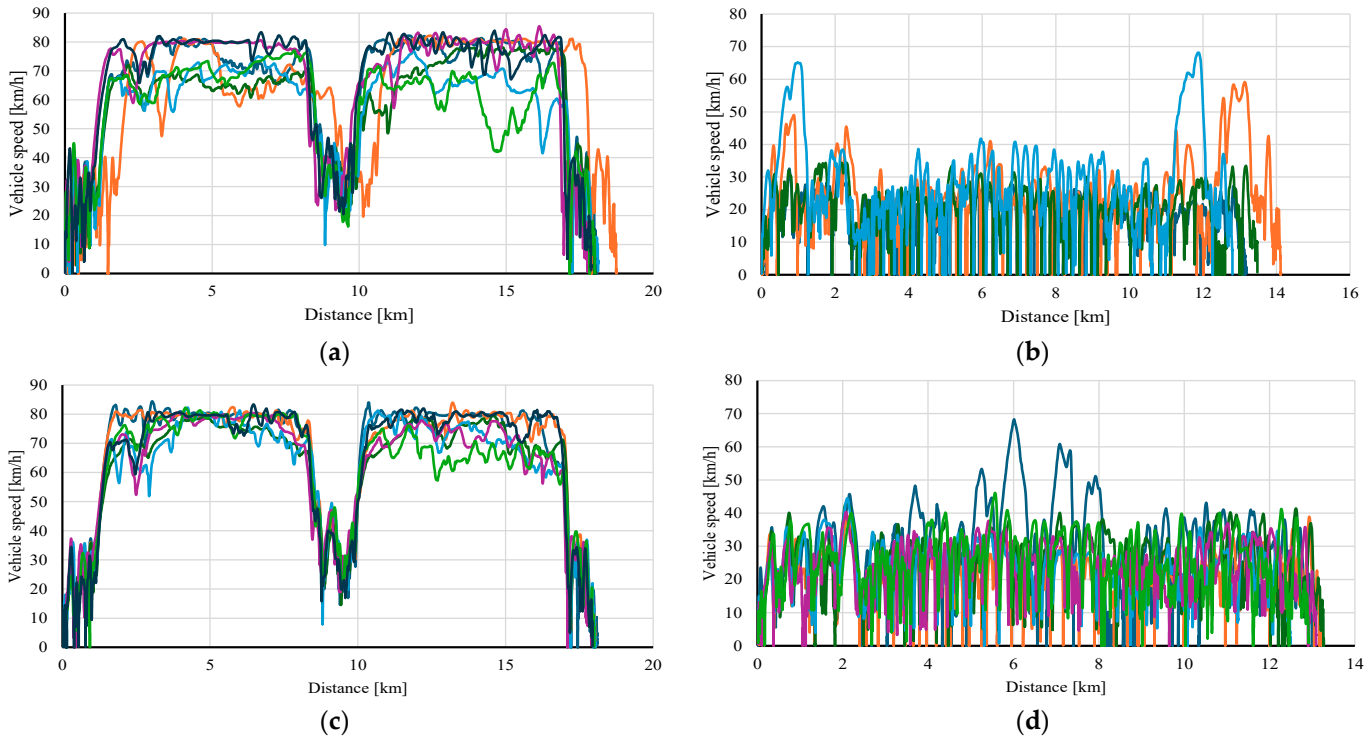

Figure 5. Vehicle's speed profiles. (**a**) Extra-urban test, CNG case; (**b**) Urban test, CNG case; (**c**) Extra-urban test, HCNG case; (**d**) Urban test, HCNG case.

It is noted that the speed profiles of the various tests within the subcategory tend to overlap. In fact, regarding the extra-urban route, it is noted that, in the initial and final stages of the journey, lower vehicle speeds are recorded because the vehicle depot is located at a certain distance from the more specifically extra-urban section. Furthermore, an average speed of 75 to 85 km/h is noted, which persists for most of the tests, except for the initial and final sections and the section between 8 and 10 km of the route.

The urban route, however, features many speed variations, with sudden accelerations and decelerations, related to the stops of the vehicle. In fact, the vehicle stalls for boarding

and alighting passengers, or due to the traffic light layout and urban traffic conditions. Speed remained under 40 km/h for most of the operating tests. Peaks exceeding 60 km/h were recorded, but only in a couple of tests. The lower vehicle's speed is evident during an urban test with respect to the extra-urban run. Speed profiles are also quite similar in terms of frequency content, reflecting the differences in the random variations due to driving.

3.2. Specific Emissions

Thanks to the on-board gas analyzer, exhaust emissions were measured and quantified during vehicle operation. The analyzer records data at 1 Hz; all samples were integrated for the entire test to obtain cumulative emissions.

All the cumulative emissions measured during the various tests carried out have been stored and subsequently elaborated, averaging them to avoid instantaneous differences also due to random situations. The results presented in this section concern the comparison of emissions for km of road travel and for kWh at the crankshaft output of energy in both extra-urban and urban environments. In addition to the average emission values, the range containing all the values with which this average was calculated is also reported.

To better interpret the results, emissions were expressed using two complementary normalization criteria. The distance-based metric (g/km) reflects real-world vehicle operation and is consistent with standard practice for passenger transport applications, enabling direct comparison among repeated tests performed under different traffic and environmental conditions. In parallel, an energy-based normalization (g/kWh) was introduced to relate emissions to the actual propulsive effort of the vehicle. This approach allows a more intrinsic evaluation of the engine performance, reducing the influence of variations in driving patterns, such as speed profiles and acceleration events.

Figure 6 presents a comparison of the emissions per km, under extra-urban driving conditions. The data has been averaged and the differences between the different tests have been reported, showing a narrow variation. Regarding CO_2 emissions, the average value is 638.6 g/km when the vehicle operates on natural gas, whereas it decreases to 575.7 g/km when hydrogen-enriched natural gas (HCNG) is used, corresponding to a reduction of 9.8% with respect to a pure methane use. More substantial emission reductions are observed with HCNG for CO, HC, and PN. In particular, the percentage reductions are equal to 25.6%, 39.8%, and 42.8%, respectively, as illustrated in Figure 6b. By contrast, averaged distance-specific NOx emissions are 15.08 g/km for natural gas operation and 15.16 g/km for HCNG operation, resulting in a slight increase of 0.47%.

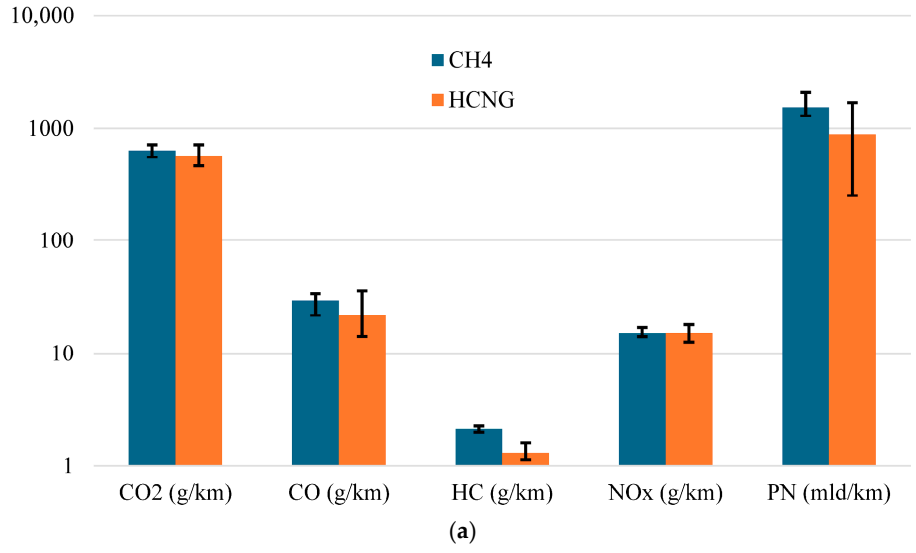

Figure 6. *Cont.*

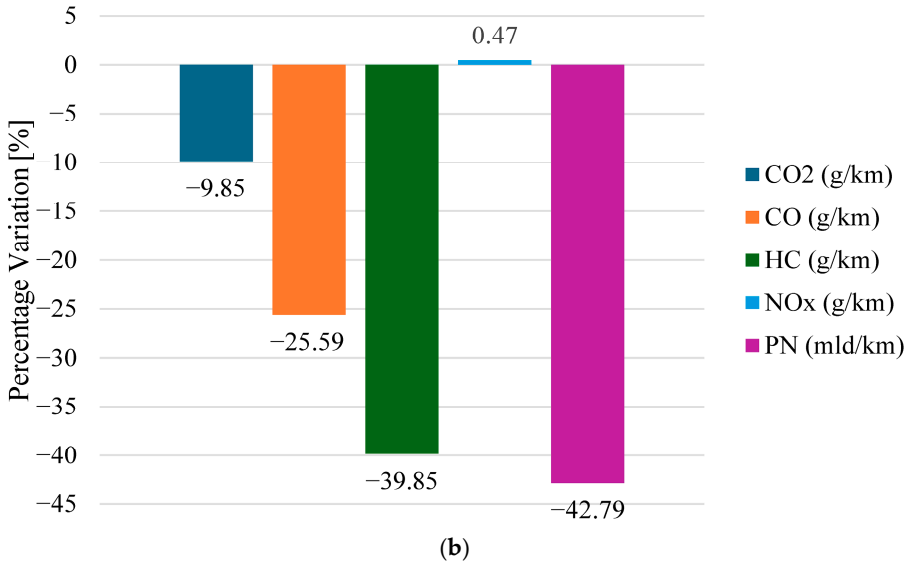

Figure 6. (**a**) Extra-urban-specific emissions (per km) and percentage variation with respect to pure methane use (**b**).

Figure 7 shows the cumulative emissions, average per kWh of propulsion energy and the percentage change when HCNG is used as fuel, compared to pure methane. Normalizing emissions to propulsion energy enables a direct relationship between emissions and the primary energy required by the propulsion system. Under this energy reference, the influence of the driving style during tests is reduced, leading to intrinsic fundamental behavior.

CO_2 emissions per kWh are nearly comparable for the two fuels. Specifically, when the vehicle operates with pure natural gas, an amount of 565.5 g/kWh is obtained slightly reduced (558.4 g/kWh) with HCNG. Also in this case, the most pronounced percentage reductions are observed for CO, HC, and PN emissions. A reduction of 18.6% for CO, 34.2% for HC, and 36.7% for PN have been assessed. By contrast, NOx emissions exhibit an increase of 10.10% due to the higher flame temperature when the HCNG is used.

A similar analysis was also carried out under urban driving conditions. In this case as well, cumulative emissions were compared for vehicle operation fed by natural gas and by hydrogen-enriched natural gas (HCNG). Figures 8 and 9 show the results per unit of distance traveled and per unit of propulsion power delivered. The same trends are evident as in the case of extra-urban driving.

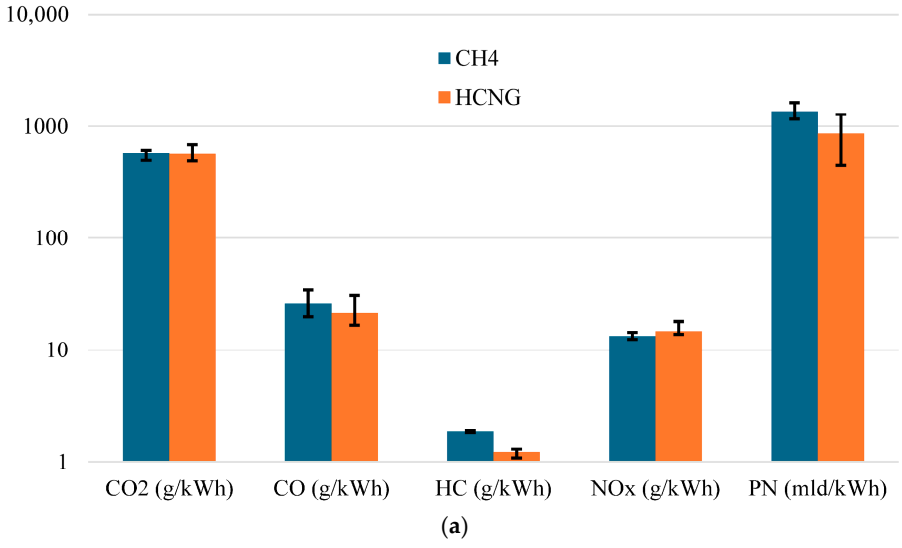

Figure 7. *Cont.*

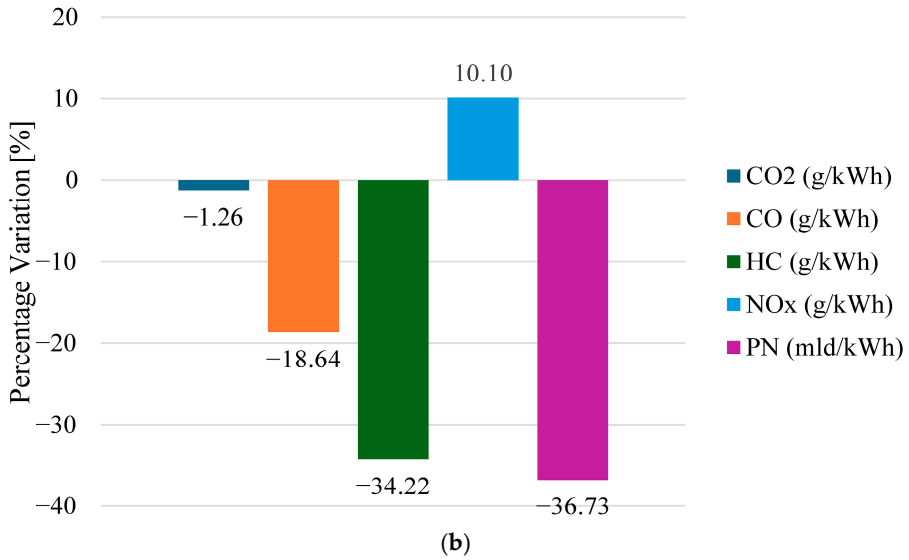

Figure 7. (**a**) Extra-urban-specific emissions referring to propulsion energy delivered a percentage variation with respect to pure methane use (**b**).

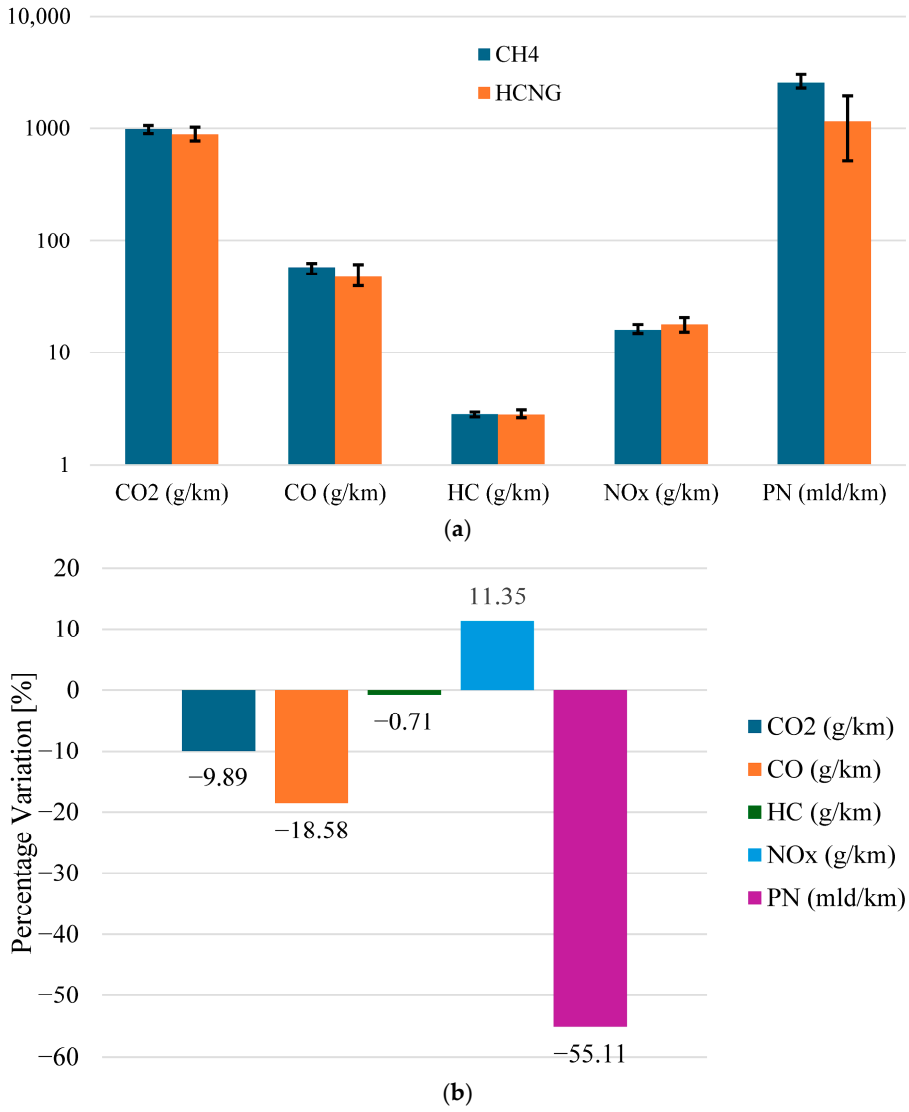

Figure 8. (**a**) Urban-specific emissions per km and percentage variation (**b**) compared to pure methane use.

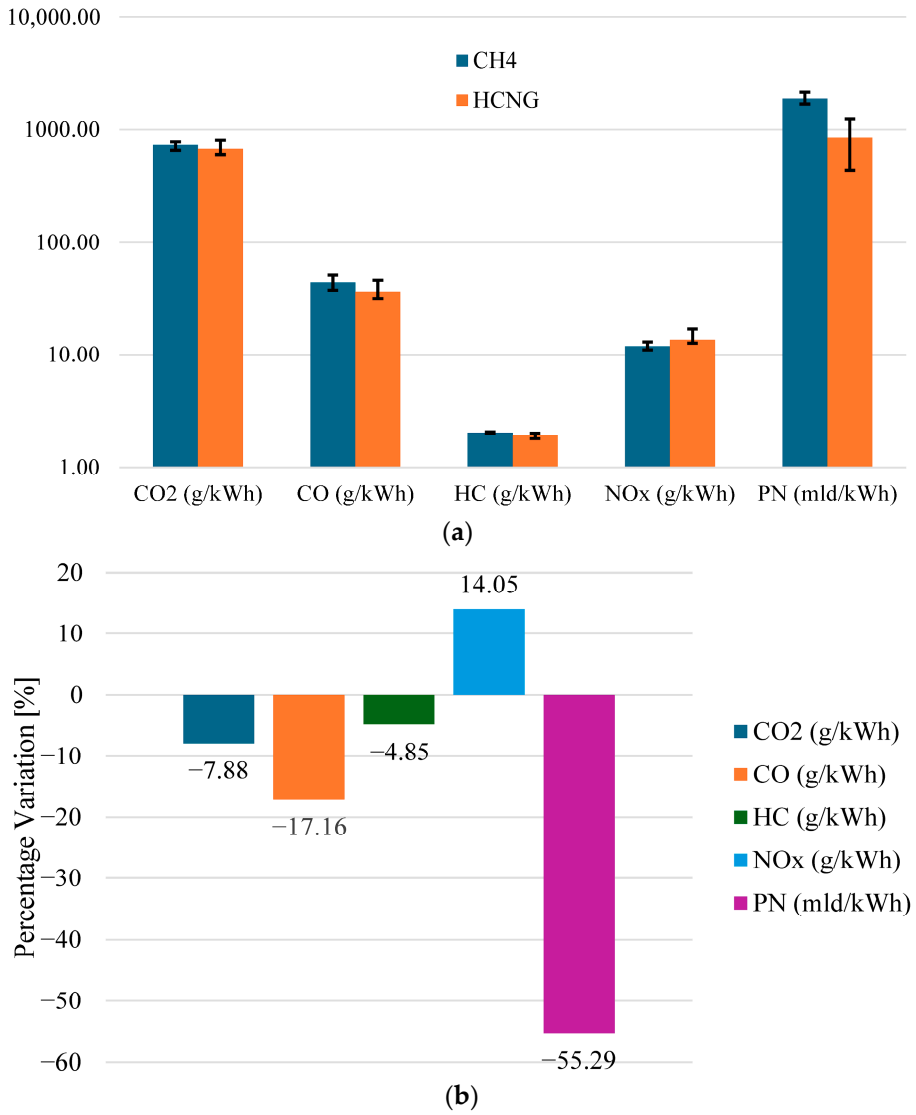

Figure 9. (**a**) Urban-specific emissions per unit of propulsion energy g/kWh and percentage variation (**b**).

More specifically, when pure methane is used, the specific emissions are: 980.1 g/km for CO_2, 58.0 g/km for CO, 2.8 g/km for HC, and 15.8 g/km for NOx, while the averaged PN emissions are equal to 2550.2 $\times$ 10^9 particles per kilometer. When the vehicle is operated on HCNG, the corresponding data is 883.2 g/km for CO_2, 47.2 g/km for CO, and 2.82 g/km for HC, whereas NOx emissions increase to 17.6 g/km; PN emissions are reduced to 1144.9 $\times$ 10^9 particles per kilometers. In terms of percentage variations with respect to pure methane, a reduction of 9.9% for CO_2, 18.6% for CO, and 0.7% for HC have been obtained. Conversely, NOx emissions exhibit a percentage increase of +11.4%, while a particularly pronounced reduction is observed for PN emissions, amounting to 55.1%.

In terms of emissions per unit of propulsion energy, the benefits when using HCNG are similarly evident. A reduction of 7.88% for CO_2, 17.16% for CO, 4.85% for HC and 55.29% for PN have been obtained while an increase of 14.05% for NOx characterizes the use of HCNG with respect to methane.

The comparison between CNG and HCNG operation highlights a general improvement in emission performance when hydrogen is introduced into the natural gas blend. CO_2 emissions show a slight reduction under HCNG operation, which can be primarily attributed to the higher hydrogen-to-carbon ratio of the fuel mixture, resulting in a lower

carbon content per unit of energy released. Even in the absence of significant efficiency variations, this fuel-related effect leads to a decrease in carbon dioxide emissions. Any moderate increase in hydrogen in the mixture can only further reduce the CO_2 emitted, making it necessary to operate on some engine variables.

A more pronounced benefit is observed for CO and unburned hydrocarbons (HCs), both of which are reduced under HCNG operation. This behavior can be further explained by the enhanced combustion characteristics induced by hydrogen addition, particularly the higher flame propagation speed and the broader flammability limits, which promote more complete oxidation processes and reduce the formation of incomplete combustion products. In parallel, particle number emissions are significantly lowered, reflecting the strong influence of hydrogen in suppressing soot precursor formation and improving overall combustion completeness, which is also relevant in engines already operating with a gaseous fuel such as CNG. In this case also, any moderate increase in the hydrogen content in the blend would reinforce the CO and HC reduction.

NO_x emissions remain broadly comparable between the two fuels, with only limited variation. This outcome can be interpreted as the result of competing effects, since hydrogen addition tends to increase local peak combustion temperatures, which would favor thermal NO_x formation, while at the same time improving mixture homogeneity and reducing rich zones, which mitigates NO_x production. The balance between these mechanisms results in an overall slight increase in NO_x emissions. Any hydrogen increase in the blend would certainly increase the NO_x emission, but a new engine set-up of the injection would make it possible to reduce it as it could be achieved by a NO_x after-treatment improvement.

In conclusion, when HCNG replaces pure methane, a clear and significant reduction in CO, CO_2, HC and PN has been obtained, particularly suitable during urban and extra-urban driving in favor of an improvement in the air quality, while, as far as NOx is concerned, a slight increase was found. Modifying the injection characteristic of the blend, the NOx increase can be managed as well as resetting the exhaust gas after treatment.

Overall, the results indicate that HCNG operation leads to a cleaner emission profile compared to CNG, mainly driven by improvements in combustion quality and fuel composition effects, thus confirming the role of hydrogen as a combustion enhancer.

3.3. Aspects Related to Fun-to-Drive and Vehicle Response

The RPA (Relative Positive Acceleration) index is a parameter used to characterize driving dynamics in real-world or test cycles [87]. It represents the amount of positive (i.e., accelerating) work per unit distance, normalized over the total trip length. In practice, it is calculated from the sum of positive accelerations multiplied by vehicle speed and divided by the distance traveled. The RPA index is widely used in emissions and energy consumption studies because it is strongly correlated with vehicle power demand, especially during transient conditions such as urban stop-and-go driving. Higher RPA values indicate more aggressive driving patterns, with frequent accelerations, leading to increased fuel consumption and pollutant emissions. Therefore, RPA is a useful metric to compare different driving routes, drivers, or traffic conditions in terms of their energy intensity and environmental impact. HCNG operation is associated with enhanced vehicle drivability, characterized by improved transient response and a more immediate engine torque delivery, which is perceived by drivers as a more responsive driving behavior.

Referring to a speed $v(t)$ and a positive acceleration $a^+(t)$ profile evaluated during a T period, and to the total distance traveled X, RPA is defined as in Equation (1):

$$RPA = \frac{1}{X}\int_0^T \left(v(t)a^+(t)\right)dt \quad (1)$$

A higher value with a pattern consisting of "valleys" and "peaks" is synonymous with more "aggressive" driving as the answer to a usual pedal variation. We chose to verify this index because the drivers of the bus reported an unconventional response of the propulsion system during their usual driving when the HCNG was used as fuel, i.e., during the usual sequences of pedals which characterized the route.

Figure 10 reports the RPA index during extra-urban driving. The index is calculated for each test deemed valid both for vehicle operation on natural gas and on hydrogen-enriched natural gas (HCNG). To verify the qualitative feedback provided by the drivers during driving, a mathematical averaging was performed on the RPA parameter, as defined in Equation (2):

$$RPA_{AV} = \frac{1}{N}\sum_{i=1}^{N} RPA \quad (2)$$

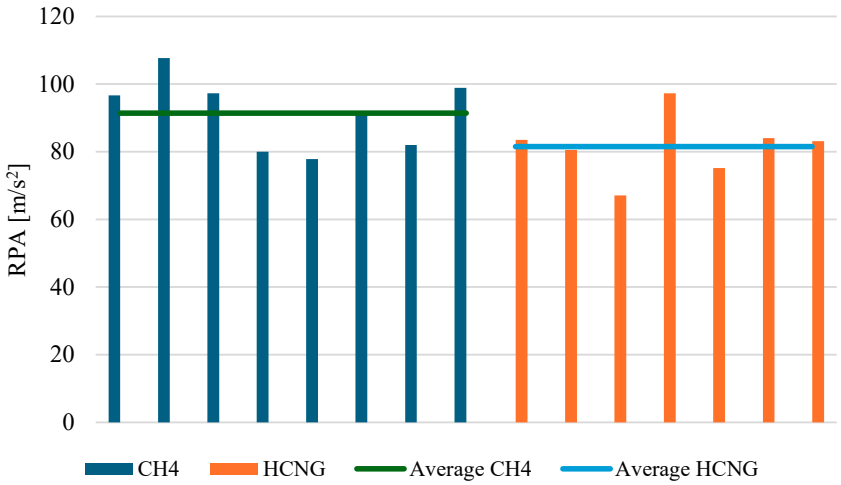

Figure 10. Extra-urban RPA values.

The average RPA values resulted equal to 81.5 m/s^2 when the bus is fueled with HCNG, whereas it is equal to 91.4 m/s^2 when the bus operates with natural gas. It should be noted that the extra-urban route is characterized by limited and infrequent variations in the vehicle speed, due to very low traffic density and a reduced number of intersections, which therefore avoid the typical speed fluctuations more typical of an urban route.

The results indicate that, when the bus is operated on HCNG, the same vehicle performance can be achieved with lower driver-demanded acceleration levels compared to CNG operation. This suggests an improved engine and drivetrain transient response, likely associated with the combustion characteristics of HCNG (faster flame speed and more stable ignition), which translate into a more immediate torque delivery and a more responsive vehicle behavior during acceleration phases.

Under urban driving conditions, the RPA index exhibits higher values compared to extra-urban operation, as shown in Figure 11. This difference is primarily attributable to the altered traffic conditions, as well as to the higher density of intersections and traffic lights, which inevitably resulted in a more irregular and discontinuous speed profile during the tests, as also evidenced by Figure 5.

Specifically, when the vehicle is operated on natural gas, the minimum and maximum RPA values are 113.7 m/s^2 and 200.7 m/s^2, respectively, with a mean arithmetic value equal to 151.8 m/s^2. Conversely, when the vehicle is fueled with hydrogen-enriched natural gas (HCNG), the RPA values fall within the range 135.8–202.2 m/s^2, with a mean value equal to 170.5 m/s^2. Both the average values and the variability range are higher than those observed under extra-urban driving conditions.

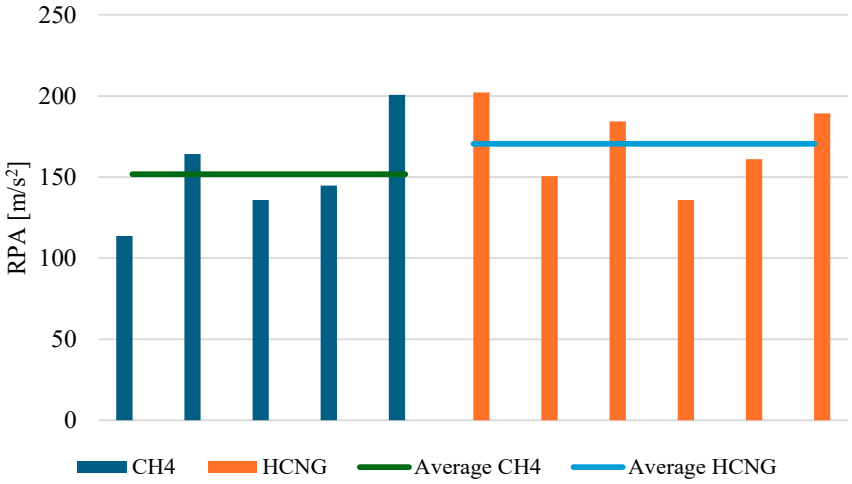

Figure 11. Urban RPA value.

These results, even though they only qualitatively corroborate the feedback provided by the drivers during the experimental campaign, always report a more responsive vehicle behavior when HCNG was used compared to natural gas. This effect can be attributed to the higher energy content introduced into the combustion chamber when operating on the hydrogen-enriched mixture, due to its higher calorific value relative to natural gas alone.

4. Conclusions

The transportation sector is increasingly required to adopt effective strategies to meet stringent sustainability targets. While electrification and hybridization represent key pathways toward decarbonization, no single solution can fully address the complexity of the transition. In this context, technologies capable of reducing fuel consumption and CO_2 emissions, together with the progressive introduction of low-carbon energy carriers, represent valuable complementary options. The use of hydrogen in internal combustion engines allows exploitation of the high technological maturity of ICEs while strongly contributing to decarbonization.

In this work, the application of a hydrogen–methane blend (HCNG) to a bus originally powered by natural gas was investigated. The intention was to sustain the efforts to improve air quality in urban areas by means of interventions which are immediately implementable and, additionally, to decrease CO_2 emissions as a contribution to decarbonization in a sector which is within those considered hard to abate. The vehicle was instrumented with a Portable Emission Measurement System to measure CO_2, CO, HC, NOx, and PN emissions under real driving conditions. Two representative routes, one urban and one extra-urban, were selected to capture typical operating conditions of the vehicle's daily mission.

Comparative tests were conducted using pure methane and an HCNG blend (15% H_2 by volume). Emissions were evaluated both on a distance basis (g/km) and on an energy basis (g/kWh), enabling a more comprehensive interpretation of the results. Across both routes, HCNG operation led to a consistent reduction in CO_2 emissions, typically in the range of approximately 3–8%, reflecting the lower carbon content of the fuel. More significant reductions were observed for incomplete combustion products, with CO and HC decreasing by about 20–40%, and particle number (PN) showing reductions on the order of one magnitude or up to 50% in some operating conditions. These trends are clearly highlighted in the emission comparison, where HCNG systematically exhibits lower levels of CO, HC, and PN compared to CNG, confirming the beneficial effect of hydrogen on combustion completeness. Conversely, NOx emissions showed a moderate increase, generally within the range of 5–15%, which can be attributed to higher in-cylinder

temperatures associated with hydrogen addition, combined with the absence of dedicated engine recalibration.

Additional insight into vehicle operation was provided by the analysis of the RPA index, which indicates that HCNG operation is associated with a more responsive vehicle behavior, requiring lower acceleration inputs to achieve the same propulsive power. This is consistent with driver feedback and can be explained by the faster combustion kinetics and improved flame propagation of hydrogen-enriched mixtures, leading to more immediate torque delivery. While this effect enhances drivability, it also suggests that optimized control strategies could further harmonize vehicle response and potentially mitigate NOx formation.

Beyond the specific experimental results, the adoption of HCNG can be framed as a partial drop-in solution for the transport sector, enabling the introduction of hydrogen without requiring substantial modifications to existing infrastructure and vehicle platforms. This represents a key advantage in the short-to-medium term, as it allows a gradual scaling of hydrogen utilization. Increasing the share of hydrogen in conventional fuels can stimulate market demand, contributing to cost reduction through economies of scale and fostering the development of more robust and structured production and distribution chains. In turn, this can lead to a progressive decrease in the carbon intensity associated with hydrogen production, especially as renewable pathways become more widespread.

Overall, the results confirm that HCNG represents an effective transitional solution to improve the environmental performance of existing natural gas vehicles, significantly reducing CO_2 and incomplete combustion emissions while maintaining acceptable NOx levels. With further optimization of engine calibration and fuel management strategies, HCNG could play a relevant role in supporting the broader deployment of hydrogen as a sustainable energy carrier in the transportation sector.

Author Contributions: Conceptualization, R.C. and D.D.B.; methodology, M.D.B., D.D.B. and F.D.P.; software, M.D.B. and F.D.P.; validation, D.D.B., M.D.B. and F.D.P.; formal analysis, D.D.B. and F.D.P.; investigation, M.D.B.; resources, R.C.; data curation, F.D.P. and M.D.B.; writing—original draft preparation, F.D.P. and D.D.B.; writing—review and editing, M.D.B. and R.C.; visualization, F.D.P.; supervision, R.C. and D.D.B.; project administration, R.C.; funding acquisition, R.C. All authors have read and agreed to the published version of the manuscript.

Funding: This research was funded by TUA S.p.A. under a specific collaboration contract.

Data Availability Statement: Dataset available on request from the authors.

Acknowledgments: AVL Italia is acknowledged for the software used in measurement testing.

Conflicts of Interest: The authors declare no conflicts of interest.

Nomenclature

Acronyms

B.E.	Brake Energy
B.P.	Brake Power
BEV	Battery Electric Vehicle
CNG	Compressed Natural Gas
CO	Carbon Monoxide
CO_2	Carbon Dioxide
DHR	Direct Heat Recovery
FC	Fuel Cell

Acronyms	
HCs	Unburned Hydrocarbons
HCNG	Enriched Compressed Natural Gas
HDV	Heavy-Duty Vehicle
ICE	Internal Combustion Engine
IHR	Indirect Heat Recovery
NCV	Net Calorific Value
NOx	Nitrogen Oxide
PN	Particle Number
RPA	Relative Positive Acceleration
WHR	Waste Heat Recovery
Symbols	
C	Torque
a	Acceleration
Cx	Vehicle's Aerodynamic Drag Coefficient
F	Force
g	Gravity Acceleration
M	Vehicle's Mass
S	Front Surface of the Vehicle
v	Vehicle's Velocity
η	Efficiency
μ	Friction Coefficient
ω	Rotational Speed
Subscript	
ae	Aerodynamics
av	Forward
AV	Average
d	Dynamic
in	Inertial
rot	Rolling

References

1. European Green Deal—Consilium. Available online: https://www.consilium.europa.eu/en/policies/green-deal/ (accessed on 12 February 2024).
2. Crippa, M.; Guizzardi, D.; Pagani, F.; Banja, M.; Muntean, M.; Schaaf, E.; Monforti-Ferrario, F.; Becker, W.E.; Quadrelli, R.; Risquez Martin, A.; et al. *GHG Emissions of All World Countries*; JRC138862; Publications Office of the European Union: Luxembourg, 2024. [CrossRef]
3. Transport and Mobility. Available online: https://www.eea.europa.eu/en/topics/in-depth/transport-and-mobility (accessed on 7 November 2024).
4. U.S. Energy Information Administration. *International Energy Outlook 2023*; U.S. Energy Information Administration: Washington, DC, USA, 2023.
5. Ritchie, H. Cars, Planes, Trains: Where Do CO_2 Emissions from Transport Come From? 2020. Available online: https://ourworldindata.org/co2-emissions-from-transport (accessed on 2 September 2024).
6. Tietge, U.; Mock, P.; Díaz, S.; Dornoff, J. CO_2 Emissions from New Passenger Cars in Europe: Car Manufacturers' Performance in 2020. *The ICCT*, 31 August 2021.
7. Krause, J.; Yugo, M.; Samaras, Z.; Edwards, S.; Fontaras, G.; Dauphin, R.; Prenninger, P.; Neugebauer, S. Well-to-wheels scenarios for 2050 carbon-neutral road transport in the EU. *J. Clean. Prod.* **2024**, *443*, 141084. [CrossRef]
8. Regulation (EU) 2024/1257 of the European Parliament and of the Council of 24 April 2024 on Type-Approval of Motor Vehicles and Engines and of Systems, Components and Separate Technical Units Intended for Such Vehicles, with Respect to Their Emissions and Battery Durability (Euro 7). Available online: https://eur-lex.europa.eu/legal-content/en/TXT/?uri=CELEX:32024R1257 (accessed on 28 April 2026).
9. Senecal, K.; Leach, F. *Racing Toward Zero: The Untold Story of Driving Green*; R-501; SAE International: Warrendale, PA, USA, 2021.

10. IEA. *Road Transport*; IEA: Paris, France, 2023. Available online: https://www.iea.org/reports/road-transport (accessed on 28 April 2026).
11. Jan, D. CO_2 Emission Standards for New Passenger Cars and Vans in the European Union. *The ICCT*, 23 May 2022.
12. Monteforte, M.; Mock, P.; Tietge, U. European Vehicle Market Statistics 2024/25. *The ICCT*, 10 December 2024.
13. Bieker, G. A Global Comparison of the Life-Cycle Greenhouse Gas Emissions of Combustion Engine and Electric Passenger Cars, White Paper. *The ICCT*. 20 July 2021. Available online: https://theicct.org/publication/a-global-comparison-of-the-life-cycle-greenhouse-gas-emissions-of-combustion-engine-and-electric-passenger-cars/ (accessed on 23 September 2025).
14. Scarlat, N.; Prussi, M.; Padella, M. Quantification of the carbon intensity of electricity produced and used in Europe. *Appl. Energy* **2022**, *305*, 117901. [CrossRef]
15. Giuliano, G.; Dessouky, M.; Dexter, S.; Fang, J.; Hu, S.; Miller, M. Heavy-duty trucks: The challenge of getting to zero. *Transp. Res. Part Transp. Environ.* **2021**, *93*, 102742. [CrossRef]
16. Bibra, E.; Connelly, E.; Dhir, S.; Drtil, M.; Henriot, P.; Hwang, I.; Marois, J.-B.; McBain, S.; Aryanpur, V.; Paoli, L.; et al. *Global EV Outlook 2022: Securing Supplies for an Electric Future*; International Energy Agency: Paris, France, 2022.
17. Olabi, A.G.; Abdelkareem, M.A.; Wilberforce, T.; Alkhalidi, A.; Salameh, T.; Abo-Khalil, A.G.; Hassan, M.M.; Sayed, E.T. Battery electric vehicles: Progress, power electronic converters, strength (S), weakness (W), opportunity (O), and threats (T). *Int. J. Thermofluids* **2022**, *16*, 100212. [CrossRef]
18. Previati, G.; Mastinu, G.; Gobbi, M. Thermal Management of Electrified Vehicles—A Review. *Energies* **2022**, *15*, 1326. [CrossRef]
19. Gundabattini, E.; Kuppan, R.; Solomon, D.G.; Kalam, A.; Kothari, D.P.; Bakar, R.A. A review on methods of finding losses and cooling methods to increase efficiency of electric machines. *Ain Shams Eng. J.* **2021**, *12*, 497–505. [CrossRef]
20. Tian, J.; Fan, Y.; Pan, T.; Zhang, X.; Yin, J.; Zhang, Q. A critical review on inconsistency mechanism, evaluation methods and improvement measures for lithium-ion battery energy storage systems. *Renew. Sustain. Energy Rev.* **2024**, *189*, 113978. [CrossRef]
21. Satrústegui, M.; Martinez-Iturralde, M.; Ramos, J.C.; Gonzalez, P.; Astarbe, G.; Elosegui, I. Design criteria for water cooled systems of induction machines. *Appl. Therm. Eng.* **2017**, *114*, 1018–1028. [CrossRef]
22. Fawzal, A.S.; Cirstea, R.M.; Gyftakis, K.N.; Woolmer, T.J.; Dickison, M.; Blundell, M. Fan Performance Analysis for Rotor Cooling of Axial Flux Permanent Magnet Machines. *IEEE Trans. Ind. Appl.* **2017**, *53*, 3295–3304. [CrossRef]
23. Di Battista, D.; Deriszadeh, A.; Di Giovine, G.; Di Prospero, F.; Cipollone, R. Modeling and Optimization of Nanofluid-Based Shaft Cooling for Automotive Electric Motors. *Energies* **2025**, *18*, 5286. [CrossRef]
24. Di Battista, D.; Bartolomeo, M.D.; Prospero, F.D.; Diomede, D.D.; Carapellucci, R.; Cipollone, R. Turbocompound energy recovery option on a turbocharged diesel engine. *J. Phys. Conf. Ser.* **2023**, *2648*, 012078. [CrossRef]
25. Winkelmann, J.; Spinler, S.; Neukirchen, T. Green transport fleet renewal using approximate dynamic programming: A case study in German heavy-duty road transportation. *Transp. Res. Part E Logist. Transp. Rev.* **2024**, *186*, 103547. [CrossRef]
26. Singh, D.V.; Pedersen, E. A review of waste heat recovery technologies for maritime applications. *Energy Convers. Manag.* **2016**, *111*, 315–328. [CrossRef]
27. Berube, M. Vehicle Technologies Office Overview. 2017. Available online: https://www.energy.gov/cmei/vehicles/annual-merit-review-presentations (accessed on 28 April 2026).
28. North American Council for Freight Efficiency (NACFE). *SUPERTRUCK 2: Empowering Future Trucking*; NACFE: Fort Wayne, IN, USA, 2024.
29. Fisher, R.; Ciappi, L.; Niknam, P.; Braimakis, K.; Karellas, S.; Frazzica, A.; Sciacovelli, A. Innovative waste heat valorisation technologies for zero-carbon ships—A review. *Appl. Therm. Eng.* **2024**, *253*, 123740. [CrossRef]
30. de Araújo, L.R.; Morawski, A.P.; Barone, M.A.; Rocha, H.R.O.; Donatelli, J.L.M.; Santos, J.J.C.S. Response surface methods based in artificial intelligence for superstructure thermoeconomic optimization of waste heat recovery systems in a large internal combustion engine. *Energy Convers. Manag.* **2022**, *271*, 116275. [CrossRef]
31. Di Battista, D.; Di Prospero, F.; Di Giovine, G.; Fatigati, F.; Cipollone, R. Dual-Stage Energy Recovery from Internal Combustion Engines. *Energies* **2025**, *18*, 623. [CrossRef]
32. Prospero, F.D.; Battista, D.D.; Cipollone, R. Model based design of a turbo-compound bottomed to internal combustion engine exhaust gas. *J. Phys. Conf. Ser.* **2024**, *2893*, 012095. [CrossRef]
33. Di Battista, D.; Cipollone, R.; Corti, E.; Brancaleoni, P.P.; Di Prospero, F.; Ravaglioli, V. *Waste Heat Recovery in Hydrogen Fueled Internal Combustion Engines*; SAE Technical Papers 2025-24-0108; SAE: Warrendale, PA, USA, 2025. [CrossRef]
34. Novotny, V.; Spale, J.; Szucs, D.J.; Tsai, H.Y.; Kolovratnik, M. Direct integration of an organic Rankine cycle into an internal combustion engine cooling system for comprehensive and simplified waste heat recovery. *Energy Rep.* **2021**, *7*, 644–656. [CrossRef]
35. Ping, X.; Yang, F.; Zhang, H.; Xing, C.; Yao, B.; Wang, Y. An outlier removal and feature dimen-sionality reduction framework with unsupervised learning and information theory intervention for organic Rankine cycle (ORC). *Energy* **2022**, *254*, 124268. [CrossRef]
36. Pili, R.; Wieland, C.; Spliethoff, H.; Haglind, F. Numerical analysis of feedforward concepts for advanced control of organic Rankine cycle systems on heavy-duty vehicles. *J. Clean. Prod.* **2022**, *351*, 131470. [CrossRef]

37. Liu, H.; Wen, M.; Yang, H.; Yue, Z.; Yao, M. A Review of Thermal Management System and Control Strategy for Automotive Engines. *J. Energy Eng.* **2021**, *147*, 03121001. [CrossRef]
38. Di Battista, D.; Di Bartolomeo, M.; Cipollone, R. The performance of engine coolant control strategies on real driving emissions. *Appl. Therm. Eng.* **2026**, *289*, 129753. [CrossRef]
39. Di Battista, D.; Di Bartolomeo, M.; Cipollone, R. Flow and thermal management of engine intake air for fuel and emissions saving. *Energy Convers. Manag.* **2018**, *173*, 46–55. [CrossRef]
40. Di Battista, D.; Deriszadeh, A.; Di Prospero, F.; Di Giovine, G.; Di Bartolomeo, M.; Fatigati, F.; Cipollone, R. *Model-Based Design and Numerical Analysis of a Downsized Centrifugal Pump for Engine Cooling Applications*; SAE Technical Paper 2025-32-0078; SAE: Warrendale, PA, USA, 2025. [CrossRef]
41. Kim, T.; Natarajan, D. *Fuel-to-Warm Methodology: Optimization Tool for Distributing Waste Heat during Warm-Up Within the Powertrain System*; SAE Technical Paper 2021-01-0210; SAE: Warrendale, PA, USA, 2021. [CrossRef]
42. Peiretti Paradisi, B.; Millo, F.; Rolando, L.; Di Battista, D.; Di Prospero, F.; Corti, E.; Brancaleoni, P.P.; Battistoni, M.; Zembi, J.; Arsie, I.; et al. Decarbonizing urban public transport: Development and final assessment of a hydrogen-fueled hybrid propulsion system for city buses. *Fuel* **2026**, *420*, 138866. [CrossRef]
43. Milojević, S.; Stopka, O.; Kontrec, N.; Orynycz, O.; Hlatká, M.; Radojković, M.; Stojanović, B. Analytical Characterization of Thermal Efficiency and Emissions from a Diesel Engine Using Diesel and Biodiesel and Its Significance for Logistics Management. *Processes* **2025**, *13*, 2124. [CrossRef]
44. UITP. An Overview of Clean Buses in Europe Clean Bus Report. January 2024. Available online: https://www.uitp.org/wp-content/uploads/sites/7/2025/04/ASSURED-Clean-Bus-report_final2.pdf (accessed on 28 April 2026).
45. Geng, P.; Cao, E.; Tan, Q.; Wei, L. Effects of alternative fuels on the combustion characteristics and emission products from diesel engines: A review. *Renew. Sustain. Energy Rev.* **2017**, *71*, 523–534. [CrossRef]
46. Guido, C.; Beatrice, C.; Di Iorio, S.; Fraioli, V.; Di Blasio, G.; Vassallo, A.; Ciaravino, C. Alternative Diesel Fuels Effects on Combustion and Emissions of an Euro5 Automotive Diesel Engine. *SAE Int. J. Fuels Lubr.* **2010**, *3*, 107–132. [CrossRef]
47. Di Blasio, G.; Ianniello, R.; Beatrice, C. Hydrotreated vegetable oil as enabler for high-efficient and ultra-low emission vehicles in the view of 2030 targets. *Fuel* **2022**, *310*, 122206. [CrossRef]
48. González Prieto, M.; Merlo Raimondi, A.; Sánchez, F.A.; Pereda, S. Simulation of phase equilibria properties of fuels and blends of fuels with oxygenated compounds. *Fuel* **2026**, *410*, 137864. [CrossRef]
49. Wouters, C.; Burkardt, P.; Steeger, F.; Fleischmann, M.; Pischinger, S. Comprehensive assessment of methanol as an alternative fuel for spark-ignition engines. *Fuel* **2023**, *340*, 127627. [CrossRef]
50. Villforth, J.; Casal, K.A.; Rossi, E.; Vacca, A.; Cupo, F.; Chiodi, M.; Bargende, M. Experimental and Numerical Identification and Optimization of eFuel Potentials on Combustion Behavior and Engine Efficiency. *Tongji Daxue Xuebao/J. Tongji Univ.* **2021**, *49*, 83–95. [CrossRef]
51. Villforth, J.; Kulzer, A.C.; Deeg, H.P.; Vacca, A.; Rossi, E.; Cupo, F.; Chiodi, M.; Bargende, M. *Methods to Investigate the Importance of eFuel Properties for Enhanced Emission and Mixture Formation*; SAE Technical Paper 2021-24-0017; SAE: Warrendale, PA, USA, 2021. [CrossRef]
52. Bicer, Y.; Dincer, I. Life cycle environmental impact assessments and comparisons of alternative fuels for clean vehicles. *Resour. Conserv. Recycl.* **2018**, *132*, 141–157. [CrossRef]
53. Nag, S.; Sharma, P.; Gupta, A.; Dhar, A. Combustion, vibration and noise analysis of hydrogen-diesel dual fuelled engine. *Fuel* **2019**, *241*, 488–494. [CrossRef]
54. Acar, C.; Dincer, I. The potential role of hydrogen as a sustainable transportation fuel to combat global warming. *Int. J. Hydrogen Energy* **2020**, *45*, 3396–3406. [CrossRef]
55. Baykara, S.Z. Hydrogen: A brief overview on its sources, production and environmental impact. *Int. J. Hydrogen Energy* **2018**, *43*, 10605–10614. [CrossRef]
56. Rameez, P.V.; Mohamed Ibrahim, M. A comprehensive review on the utilization of hydrogen in low temperature combustion strategies: Combustion, performance and emission attributes. *J. Energy Inst.* **2024**, *113*, 101511. [CrossRef]
57. Misra, A.; Yadav, M.; Sharma, A.; Singh, G. Methane–Diesel Dual Fuel Engine: A Comprehensive Review. In *Proceedings of International Conference in Mechanical and Energy Technology. Smart Innovation, Systems and Technologies*; Yadav, S., Singh, D., Arora, P., Kumar, H., Eds.; Springer: Singapore, 2020; Volume 174. [CrossRef]
58. Ram, V.; Salkuti, S.R. An Overview of Major Synthetic Fuels. *Energies* **2023**, *16*, 2834. [CrossRef]
59. Bonah Agyekum, E.; Odoi-Yorke, F.; Abeley Abbey, A.; Kafui Ayetor, G. A review of the trends, evolution, and future research prospects of hydrogen fuel cells—A focus on vehicles. *Int. J. Hydrogen Energy* **2024**, *72*, 918–939. [CrossRef]

60. Taskin, J.; Shafiullah, G.M.; Dawood, F.; Kaur, A.; Arif, M.T.; Pugazhendhi, R.; Elavarasan, R.M.; Forruque, S.A. Fuelling thefuture: An in-depth review of recent trends, challenges and opportunities of hydrogen fuel cell for a sustainable hydrogen economy. *Energy Rep.* **2023**, *72*, 2103–2127. [CrossRef]
61. Lixin, F.; Zhengkai, T.; Siew, H.C. Recent development of hydrogen and fuel cell technologies: A review. *Energy Rep.* **2021**, *7*, 8421–8446. [CrossRef]
62. Brancaleoni, P.P.; Corti, E.; Di Prospero, F.; Di Battista, D.; Cipollone, R.; Ravaglioli, V. Optimization of Hydrogen Internal Combustion Engines Equipped with Turbocompound Technology for Enhanced Performance and Efficiency. *Energies* **2025**, *18*, 2166. [CrossRef]
63. European Hydrogen Observatory. Available online: https://observatory.clean-hydrogen.europa.eu/index.php/hydrogen-landscape/end-use/hydrogen-fuel-cell-electric-vehicles (accessed on 3 January 2024).
64. Statista. Global Hydrogen Fuel Cell Electric Vehicle Sales in 2023, by Country or Region. Available online: https://www.statista.com/statistics/1454512/annual-fcev-sales-by-country-or-region/ (accessed on 3 January 2024).
65. Pramuanjaroenkij, A.; Kakaç, S. The fuel cell electric vehicles: The highlight review. *Int. J. Hydrogen Energy* **2023**, *48*, 9401–9425. [CrossRef]
66. Gómez, J.; Santos, D. The Status of On-Board Hydrogen Storage in Fuel Cell Electric Vehicles. *Designs* **2023**, *7*, 97. [CrossRef]
67. International Energy Agency. *Global Hydrogen Review 2023*; IEA: Paris, France, 2021. Available online: https://www.iea.org/reports/global-hydrogen-review-2023 (accessed on 12 February 2024).
68. Habib, M.A.; Abdulrahman, G.A.Q.; Alquaity, A.B.S.; Qasem, N.A.A. Hydrogen combustion, production, and applications: A review. *Alex. Eng. J.* **2024**, *100*, 182–207. [CrossRef]
69. Yip, H.L.; Srna, A.; Yuen, A.C.Y.; Kook, S.; Taylor, R.A.; Yeoh, G.H.; Medwell, P.R.; Chan, Q.N. A Review of Hydrogen Direct Injection for Internal Combustion Engines: Towards Carbon-Free Combustion. *Appl. Sci.* **2019**, *9*, 4842. [CrossRef]
70. Mahajan, D.; Tan, K.; Venkatesh, T.; Kileti, P.; Clayton, C.R. Hydrogen Blending in Gas Pipeline Networks—A Review. *Energies* **2022**, *15*, 3582. [CrossRef]
71. No, S.; Gu, J.; Moon, H.; Lee, C.; Jo, Y. *An Introduction to Combustion Concepts and Applications*; McGraw-Hill: Seoul, Republic of Korea, 2011.
72. Papagiannakis, R.G.; Hountalas, D.T. Combustion and exhaust emission characteristics of a dual fuel compression ignition engine operated with pilot diesel fuel and natural gas. *Energy Convers. Manag.* **2004**, *45*, 2971–2987. [CrossRef]
73. Ma, F.; Ding, S.; Wang, Y.; Wang, Y.; Wang, J.; Zhao, S. Study on combustion behaviors and cycle-bycycle variations in a turbocharged lean burn natural gas SI engine with hydrogen enrichment. *Int. J. Hydrogen Energy* **2008**, *33*, 7245–7255. [CrossRef]
74. Karim, G.A. Hydrogen as a spark ignition engine fuel. *Int. J. Hydrogen Energy* **2003**, *28*, 569–577. [CrossRef]
75. Bielaczyc, P.; Woodburn, J.; Szczotka, A. An assessment of regulated emissions and CO_2 emissions from a European light-duty CNG-fueled vehicle in the context of Euro 6 emissions regulations. *Appl. Energy* **2014**, *117*, 134–141. [CrossRef]
76. Gioria, R.; Selleri, T.; Giechaskiel, B.; Franzetti, J.; Ferrarese, C.; Melas, A.; Forloni, F.; Suarez-Bertoa, R.; Perujo, A. Regulated and unregulated emissions from Euro VI Diesel and CNG heavy-duty vehicles. *Transp. Res. Part D Transp. Environ.* **2024**, *134*, 104349. [CrossRef]
77. Verhelst, S.; Wallner, T. Hydrogen-fueled internal combustion engines. *Prog. Energy Combust. Sci.* **2009**, *35*, 490–527. [CrossRef]
78. Zareei, J.; Yusoff Ali, H.; Abdullah, S.; Wan Mahmood, W.M.F. Comparing the effects of hydrogen addition on performance and exhaust emission in a spark ignition fueled with gasoline and CNG. *Appl. Mech. Mater.* **2012**, *165*, 120–124. [CrossRef]
79. Banapurmath, N.R.; Gireesh, N.M.; Basavarajappa, Y.H.; Hosmath, R.S.; Yaliwal, V.S.; Pai, A.; Navale, K.P.; Jog, P.; Tewari, P.G. Effect of hydrogen addition to CNG in a biodiesel-operated dual-fuel engine. *Int. J. Sustain. Eng.* **2015**, *8*, 332–340. [CrossRef]
80. Agarwal, A.K.; Agarwal, R.A.; Gupta, T.; Gurjar, B.R. *Biofuels: Technology, Challenges and Prospects*; Springer: Singapore, 2017. [CrossRef]
81. Prasad, R.K.; Agarwal, A.K. Development and comparative experimental investigations of laser plasma and spark plasma ignited hydrogen enriched compressed natural gas fueled engine. *Energy* **2021**, *216*, 119282. [CrossRef]
82. Hora, T.S.; Agarwal, A.K. Effect of varying compression ratio on combustion, performance, and emissions of a hydrogen enriched compressed natural gas fuelled engine. *J. Nat. Gas Sci. Eng.* **2016**, *31*, 819–828. [CrossRef]
83. Sagar, S.M.V.; Agarwal, A.K. Experimental investigation of varying composition of HCNG on performance and combustion characteristics of a SI engine. *Int. J. Hydrogen Energy* **2017**, *42*, 13234–13244. [CrossRef]
84. Baratta, M.; D'Ambrosio, S.; Misul, D.A. *Performance and Emissions of a Turbocharged Spark Ignition Engine Fuelled with CNG and CNG/Hydrogen Blends*; SAE Technical Paper 2013-01-0866; SAE: Warrendale, PA, USA, 2013. [CrossRef]
85. Sutar, P.; Sekhar, R.; Thipse, S.; Rairikar, S.; Sonawane, S.; Bandyopadhyay, D. Cycle-to-Cycle Combustion Stability Evaluation of HCNG Blends in Multi-Cylinder Engines via Coefficient of Variation Analysis. *J. Eur. Syst. Autom.* **2025**, *58*, 791–803. [CrossRef]

86. Ma, F.; Wang, Y.; Liu, H.; Li, Y.; Wang, J.; Ding, S. Effects of hydrogen addition on cycle-by-cycle variations in a lean burn natural gas spark-ignition engine. *Int. J. Hydrogen Energy* **2008**, *33*, 823–831. [CrossRef]
87. D'Agostino, V.; Verdone, G.; Cardone, M. An Overview about FPT Industrial Telematic Service for Monitoring and Diagnostic purposes. First approaches to Signal Logger Data from Heavy-Duty Commercial Vehicles. *J. Phys. Conf. Ser.* **2024**, *2893*, 012106. [CrossRef]